CO and C_2 excited states relaxation in CO_2 plasmas derived from a Collisional-Radiative model

Arnaud Bultel[1], Ioan F. Schneider[2] and Yacine Babou[3]

[1]UMR CNRS 6614 CORIA, Université de Rouen, Avenue de l'Université, BP12, 76801 Saint-Etienne du Rouvray, France
[2]FRE 3102 LOMC, Université du Havre, BP 540, rue Philippe Lebon, 76058 Le Havre, France
[3]Von Karman Institute, Chaussée de Waterloo, 72 B-1640 Rhode Saint-Genèse, Belgium

E-mail: arnaud.bultel@coria.fr

Abstract. In order to explain the behavior of the main excited electronic states of CO and C_2 molecules formed in CO_2 entry or ground test facilities plasmas, a time-dependent Collisional-Radiative (CR) model is elaborated. This CR model is then included in the general balance equation of the species to give an insight on the influence of the transport and elementary processes. The related flows are generally observed under relatively low temperature owing to the numerous internal degrees of freedom to be excited, leading to a rather weak ionization degree. The electron-induced processes are even so taken into account: their influence is studied and commented. The conditions to reach non-equilibrium steady states and the related characteristic time scales are discussed as well.

1. Introduction

The important increase of the translation temperature during the atmospheric entry of a vehicle leads to the formation of a plasma characterized by numerous electronic excited species [1]. Conversely to the case of Earth's re-entries where nitrogen and oxygen lead to the formation of weakly radiative species, the case of Martian entries can be dramatic since the species formed are CO, C_2 and CN which radiate strongly [2]. The net heat flux density to the vehicle's wall can be strongly increased and damage it in part. One of the challenges of ground studies is to identify the kinetic mechanism leading to the formation of the states involved and to estimate their population density [3]. In this communication, we present a Collisional-Radiative (CR) model devoted to the theoretical study of the relaxation of the CO and C_2 main electronic states in the case of the pure CO_2 plasmas obtained in the ground test facilities (ICP torches) of VKI and CORIA institutes. This model takes into account the main processes leading to population densities changes by collisions (excitation/deexcitation, dissociation/recombination, exchange processes under heavies or electron impact) and radiation (spontaneous emission).

2. Species and CO and C_2 states involved

Owing to the possible dissociation of CO_2 under high temperature levels, CO and O can be formed. These species can re-associate to form O_2 and C_2 whose dissociation can produce C. The mixture is therefore composed by the following six species CO_2, CO, O_2, C_2, C and O. The collisions between them can lead to the CO and C_2 electronic states excitation whose less

excited ones can modify the behavior of the flow since they may be sufficiently populated. These states are listed in table 1.

Table 1. CO and C_2 states considered and their spectroscopic constants with usual notations [4].

CO No	State	g_e	T_e (eV)	ω_e (eV)	$\omega_e x_e$ (10^{-3}eV)	B_e (10^{-4}eV)	E_{diss} (eV)	Dissociation state
1	$X^1\Sigma^+$	1	0.000	0.2690	1.648	2.395	11.092	C(^{3}P)+O(^{3}P)
2	$a^3\Pi$	6	6.036	0.2162	1.780	2.097	5.082	C(^{3}P)+O(^{3}P)
3	$a'^3\Sigma^+$	3	6.921	0.1523	1.298	1.667	4.229	C(^{3}P)+O(^{3}P)
4	$d^3\Delta_i$	6	7.578	0.1453	1.319	1.625	3.576	C(^{3}P)+O(^{3}P)
5	$e^3\Sigma^-$	3	7.964	0.1386	1.325	1.591	3.193	C(^{3}P)+O(^{3}P)
6	$A^1\Pi$	2	8.068	0.1882	2.405	1.998	3.065	C(^{3}P)+O(^{3}P)
7	$D^1\Delta^-$	2	8.174	0.1356	1.265	1.558	2.985	C(^{3}P)+O(^{3}P)
8	$b^3\Sigma^+$	3	10.392	0.2727	1.860	2.462	0.698	C(^{3}P)+O(^{3}P)
9	$B^1\Sigma^+$	1	10.780	0.2619	1.887	2.432	0.316	C(^{3}P)+O(^{3}P)
C_2 No	State	g_e	T_e (eV)	ω_e (eV)	$\omega_e x_e$ (10^{-3}eV)	B_e (10^{-4}eV)	E_{diss} (eV)	Dissociation state
10	$X^1\Sigma_g^+$	1	0.000	0.2300	1.654	2.256	6.210	C(^{3}P)+C(^{3}P)
11	$a^3\Pi_u$	6	0.089	0.2035	1.447	2.024	6.134	C(^{3}P)+C(^{3}P)
12	$b^3\Sigma_g^-$	3	0.798	0.1823	1.387	1.858	5.436	C(^{3}P)+C(^{3}P)
13	$A^1\Pi_u$	2	1.040	0.1994	1.497	2.004	5.185	C(^{3}P)+C(^{3}P)
14	$c^3\Sigma_u^+$	3	1.650	0.2432	1.699	2.319	4.553	C(^{3}P)+C(^{3}P)
15	$d^3\Pi_g$	6	2.432	0.2217	2.038	2.173	3.732	C(^{3}P)+C(^{3}P)
16	$C^1\Pi_g$	2	4.248	0.2243	1.960	2.211	4.493	C(^{1}D)+C(^{1}D)
17	$e^3\Pi_g$	6	5.058	0.1372	4.868	1.478	2.462	C(^{3}P)+C(^{1}P)
18	$D^1\Sigma_u^+$	1	5.361	0.2268	1.728	2.273	4.799	C(^{1}D)+C(^{1}S)

3. CR model and balance equation

The behavior of these excited species is governed by the general balance equation, which is given under the following form:

$$\frac{\partial[X_i]}{\partial t} = -\vec{\nabla}\left([X_i]\,\vec{v}\right) - \vec{\nabla}\vec{J}_{X_i} + \left(\frac{\partial[X_i]}{\partial t}\right)_{Rad.} + \left(\frac{\partial[X_i]}{\partial t}\right)_{Coll.} \quad (1)$$

with in the right-hand side the convective, diffusive, radiative and collisional terms respectively. The elaboration of the CR model consists in calculating realistically the elementary processes involved in the collisional and radiative terms. (1) can be modified to derive a first order differential equation. The diffusion is mainly due to the fundamental diffusion mode depending on the diffusion coefficient $\bar{D}_{X_i}$ and the characteristic radius R of the flow. In addition, the convection term can be crudely estimated by R and v. We have stated:

$$\vec{\nabla}\left([X_i]\,\vec{v}\right) \approx v\,\frac{[X_i]}{R} \qquad \text{and} \qquad \vec{\nabla}\vec{J}_{X_i} = \bar{D}_{X_i}\,\frac{[X_i]}{L_0^2} \qquad \text{with} \qquad L_0 = \frac{R}{2.405} \tag{2}$$

The radiative term of (1) takes into account the main radiative systems listed in table 2. Radiation produced during spontaneous emission can be trapped owing to the opacity of the flow. An escape factor denoted $\Lambda_{j\to i}$ depending both on the upper j and lower i transition level densities is calculated assuming a global Doppler line broadening under the form:

$$\Lambda_{j\to i} = e^{-\frac{k_0^{j\to i}\,R}{(k_0\,R)_{ref}}} \qquad \text{with} \qquad (k_0\,R)_{ref} = 1.587 \tag{3}$$

where $k_0^{j\to i}$ is the emission coefficient by unit length at the line center for the transition $j \to i$.

With this escape factor, the $j \to i$ system contribution to $(\partial[X_i]/\partial t)_{Rad.}$ and $(\partial[X_j]/\partial t)_{Rad.}$ is:

$$\left(\frac{\partial[X_i]}{\partial t}\right)_{Coll.}^{(j\to i)} = +\Lambda_{j\to i}\,\frac{[X_j]}{\tau_{j\to i}} \qquad \text{and} \qquad \left(\frac{\partial[X_j]}{\partial t}\right)_{Coll.}^{(j\to i)} = -\Lambda_{j\to i}\,\frac{[X_j]}{\tau_{j\to i}} \tag{4}$$

The collisional term is classical and accounts for the usual (excitation/deexcitation, dissociation/recombination, exchange) processes under both heavies and electron impact. The rate coefficients used can be found in [8, 9, 10, 11, 12, 13]. The review of data derived from literature can be found in [14]. The forward processes are not only accounted for: the backward rate coefficients are also included and their values are derived from the forward ones using the detailed balance principle.

Finally the heavy particles are assumed under Maxwellian equilibrium according to a temperature denoted T_A and the electrons with their own temperature denoted T_e. The ordinary differential equations system obtained is solved by using the DVODE library [15].

Table 2. CO and C_2 main radiative systems taken into account in (1) and the related lifetimes τ [5, 6, 7].

CO transition (j→ i)	System	$\tau_{j\to i}$ (ns)	C_2 transition (j→ i)	System	$\tau_{j\to i}$ (ns)
$a'^3\Sigma^+ \to a^3\Pi$	Asundi	10^5	$A^1\Pi_u \to X^1\Sigma_g^+$	Philips	13×10^3
$d^3\Delta_i \to a^3\Pi$	Triplet	250	$D^1\Sigma_u^+ \to X^1\Sigma_g^+$	Mulliken	13
$A^1\Pi \to X^1\Sigma^+$	4^{th} positive	10	$C^1\Pi_g \to A^1\Pi_u$	Deslandres-d'Azambuja	28
$b^3\Sigma^+ \to a^3\Pi$	3^{rd} positive	54	$b^3\Sigma_g^- \to a^3\Pi_u$	Ballik and Ramsay	17×10^3
$B^1\Sigma^+ \to X^1\Sigma^+$	Hopfield-Birge	94	$d^3\Pi_g \to a^3\Pi_u$	Swan	102
$B^1\Sigma^+ \to A^1\Pi$	Angstrøm	50	$e^3\Pi_g \to a^3\Pi_u$	Fox-Herzberg	200

4. Results

The test-case studied is related to typical conditions obtained in plasma torches of the VKI and CORIA institutes: $T_A = 8000$ K, $T_e = 10000$ K, $p = 1500$ Pa, $v = 200$ m s^{-1} and $R = 4$ cm. Successive assumptions are stated in order to identify the cause of departure from equilibrium and to assess the influence of electrons.

Figure 1 illustrates the time evolution of the population densities starting from particular initial state when radiation and electron-induced processes are disregarded. We can notice the relative rapid evolution of these densities until a steady state obtained for $\tau = 0.4{\times}10^{-6}$ s. The calculation of the excitation temperature of a level i based on the ground state by:

$$T_{exc}(i) = \frac{E(i) - E(X)}{k_B} \left\{ \ln \left(\frac{g_e(i)}{g_e(X)} \frac{Z_{rv}(i)}{Z_{rv}(X)} \frac{[X]}{[i]} \right) \right\}^{-1} \tag{5}$$

provides information on additional characteristics of the final steady state. As we can see on figure 2, all excitation temperatures are equal to T_A at the final stage of the evolution. The diffusion and convective exchanges have no influence in this case. This means that the mixture is in chemical equilibrium: the population densities only depend on the local conditions. We have performed other calculations with different initial conditions. In each case, the final steady state is the same, proving without any doubt that this final state is indeed an equilibrium state.

The time needed to reach the final equilibrium state depends mainly on T_A and the pressure level p such that the following law can be derived:

$$\tau_{eq} = \frac{9.44}{p\, T_A^{1.0177}} \tag{6}$$

We can therefore assume in a first approximation that the product $\tau_{eq}\, p\, T_A$ is constant.

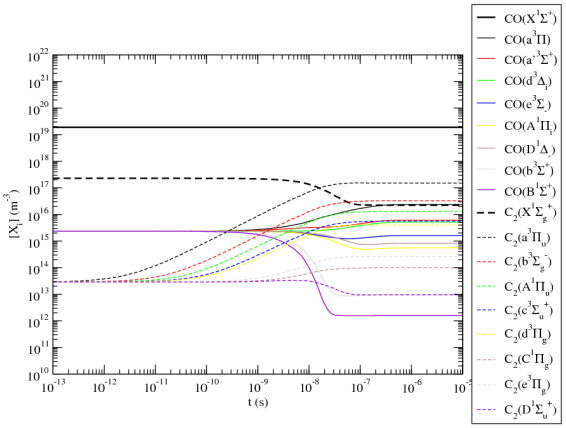

Figure 1. Population densities time-evolution starting from specific conditions without radiation.

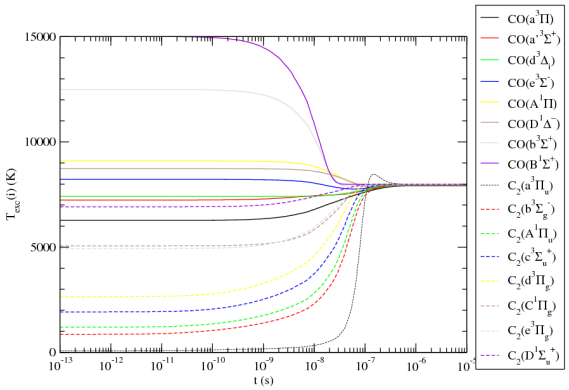

Figure 2. Excitation temperatures calculated by equation 5 in the conditions of figure 1.

These behaviours are no longer observed when the radiative processes are included in $(\partial[X_i]/\partial t)_{Rad.}$. Figure 3 displays the time-evolution of the population densities and figure 4 the time-evolution of the $\Lambda_{j\to i}$ terms: in this case, the mixture is almost optically thin.

A steady state is clearly observed, but the final excitation temperatures do not correspond to T_A. We can conclude that this steady state is not an equilibrium state. In figure 5 are also displayed the results obtained by changing the initial conditions. In both cases, the time needed to reach the steady state is approximately the same: 0.5×10^{-6} s. Its order of magnitude is remarkably close to the one obtained without considering radiative processes. This similar order of magnitude added to the near optically thin character of the flow explain why a final non equilibrium state is observed. If the pressure is higher, (6) indicates that the time needed to obtain equilibrium is shorter. In this case, the lower states population density is higher which leads to a higher optical thickness of the flow: the mixture is therefore quickly in equilibrium. In

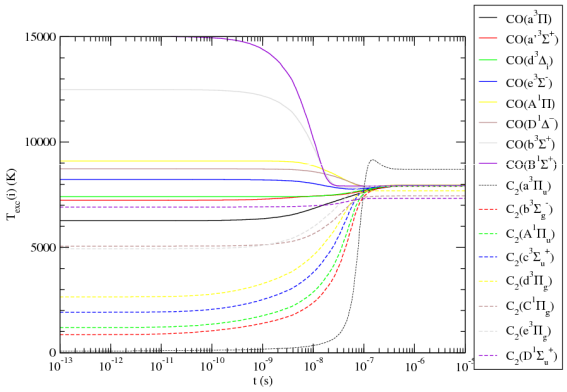

Figure 3. Excitation temperatures time-evolution including radiation (same conditions and initial state as for figures 1 and 2).

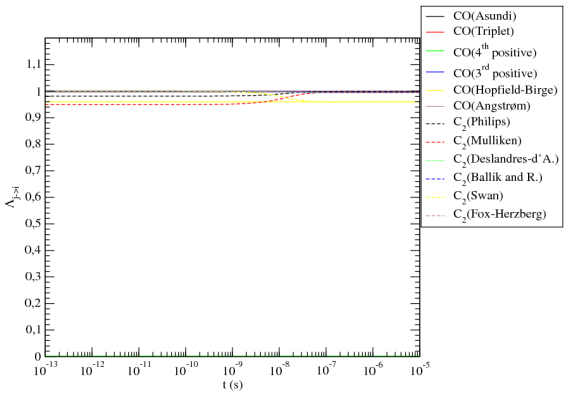

Figure 4. Time-evolution of the radiative systems escape factor. We can notice that $\lim_{t\to\infty} \Lambda_{j\to i} \approx 1$: the mixture is globally optically thin.

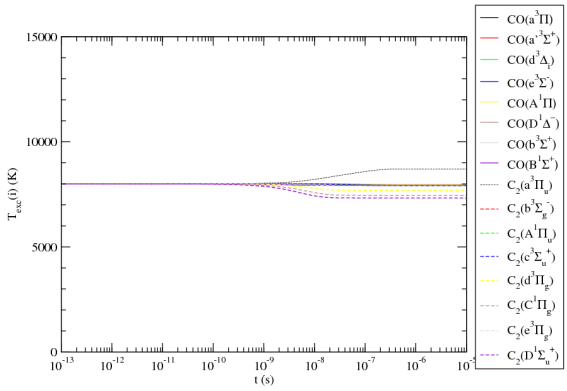

Figure 5. Same as figure 3, but with different initial conditions corresponding to an excitation equilibrium at $T_{exc} = 8000$ K.

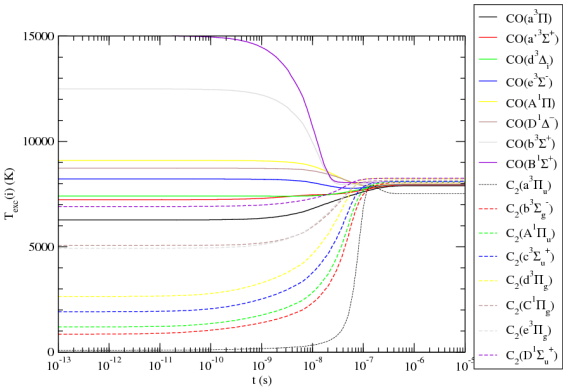

Figure 6. Excitation temperatures time-evolution with radiation and electron-induced processes (same conditions and initial state as for figures 1 and 2).

the contrary case, the mixture is closer to an optically thin medium whose radiation can easily escape according to a time scale logically given by the mean radiative lifetimes reported in table 2. The mixture cannot be longer considered as isolated: the final steady state is therefore a non equilibrium state (case of figures 3, 4 and 5).

CO and C_2 seem to present different behaviors. Carbon monoxide is much more close to equilibrium, contrary to the case of C_2. It is difficult to ascribe the difference to the radiative lifetimes values. These differences remain an open question so far and necessitate further studies.

In ICP torches, the production of the plasma results from an alternative orthoradial electromagnetic field which accelerates the statistically existing electrons in the injected gas and induces ionization phenomena under electron impact: in this area, n_e and T_e are therefore rather strong. Flowing from this zone and recombining owing to energy losses, the plasma is characterized by decreasing electron parameters. Despite this recombination, n_e and T_e can be high enough downstream to influence the chemistry. We have therefore also included electrons in the elementary processes of (1).

Assuming $T_e > T_A$ owing to the creation mode described above ($T_e = 10000$ K), we have

searched for the minimum n_e value to obtain departures from the previous behaviors. Figure 6 illustrates the results when $n_e = 10^{19}$ m^{-3} which corresponds to an ionization degree of 0.1. We can notice that C_2 presents a different behavior from CO again: we have to further analyze the situation to explain why this difference is observed. Nevertheless, this threshold is interesting. This electron density is rather high and is presumed difficult to be reached in the case of CO_2 flows: numerous degrees of freedom have indeed to be excited to dissociate the molecule, which leads certainly to a lower n_e value. We can therefore state that the electron-induced processes play a negligible role in the present conditions.

In the case of the plasmas obtained during a Martian entry phase, the pressure level behind the shock front is largely higher than the one considered previously owing to the high compression of the hypersonic flow [16]. We can reasonably assume valid (6) if the influence of N_2 can be considered as negligible[1]. In this case, the time required to reach equilibrium is very short. Departure from equilibrium can therefore only be expected in the boundary layer surrounding the object's surface.

5. Conclusion

A Collisional-Radiative model is elaborated in order to give an insight of the behavior of the CO and C_2 excited states in the conditions of the ground test facilities of VKI and CORIA institutes. Departures from equilibrium can be ascribed to radiative losses mainly. Electron-induced processes can be considered obviously as negligible. CO and C_2 do not have the same behavior: the reasons for such discrepancies have not been yet identified and necessitate further developments.

Acknowledgments

The authors wish to thank the IEFE French Institute (Institut Energie, Fluide & Environnement) for its financial support.

References

[1] Zel'dovich Ya B and Raizer Yu P 2002 *Physics of shock waves and high-temperature hydrodynamic phenomena* Hayes W.D. and Probstein R.F. Mineola, N.Y. (Dover Publications)
[2] Bultel A, Rond C, Boubert P and Chéron B G 2008 *Proc. Int. Work. Radiation of High Temperature Gases in Atmospheric Entry* ESA p32
[3] Bultel A, Chéron B G, Bourdon A, Motapon O and Schneider I F 2006 *Phys. Plasmas* **13** 043502
[4] Capitelli M, Colonna G, Giordano D, Marraffa L, Casavola A, Minelli P, Pagano D, Pietanza L D and Taccogna F 2005 *Tables of internal partition functions and thermodynamic properties of high-temperature properties of high-temperature Mars-atmosphere species from 50K to 50000K* ed D Giordano and B Warmstein (ESA STR-246)
[5] Babou Y 2007 *Ph.D Thesis* University Paris-Sud Orsay, France
[6] Da Silva M L 2004 *Ph.D Thesis* University of Orleans, France
[7] Kirby K and Cooper D L 1989 *J. Chem. Phys.* **90** 4895-4902
[8] Bauer W, Becker K H, Bielefeld M and Meuser R 1986 *Chem. Phys. Lett.* **123** 33-36
[9] Becker K H, Donner B, Freitas Dinis C M, Geiger H, Schmidt F and Wiesen P 2000 *Zeitschrift fur Physikalische Chemie* **214** 503-510
[10] Gorse C, Cacciatore M and Capitelli M 1984 *Chem. Phys.* **85** 165-176
[11] Mangir M S, Reisler H and Wittig C 1980 *J. Chem. Phys.* **73** 829-835
[12] Surzhikov S 2008 *Proc. VKI Lecture Series* RTO-EN-AVT-162
[13] Zalogin G N, Kozlov P V, Kuznetsova L A, Losev S A, Makarov V N and Romanenko Yu V 2001 *Technical Physics* **46** 10-16
[14] Bultel A 2009 *Elaboration de codes modèles collisionnels-radiatifs électroniques spécifiques portant sur CO et C_2* CORIA Technical Note
[15] Brown P N, Byrne G D and Hindmarsh A C 1989 *SIAM J. Scient. Comput.* **10** 1038
[16] Park C, Howe J T, Jaffe R L, Candler G V 1994 *J. Thermophys. Heat Transfer* **8** 1, 9-23

[1] The relative CO_2-N_2-Ar composition of the Martian atmosphere is 95%-3%-1.6%.